Liquefaction-induced damage assessment in Gölbaşı city after the 6th February 2023 Türkiye earthquakes

Michela Pulsoni [i], Anna Chiaradonna[ii], Alper Sezer [iii] and Paola Monaco[iv]

i) Master Student, University of L'Aquila, Dept. of Civil, Construction-Architectural and Environmental Engineering, Piazzale Ernesto Pontieri 1 – Monteluco di Roio, 67100 L'Aquila, Italy
ii) Research Assistant, University of L'Aquila, Dept. of Civil, Construction-Architectural and Environmental Engineering, Piazzale Ernesto Pontieri 1 – Monteluco di Roio, 67100 L'Aquila, Italy
iii) Professor, Ege Üniversitesi, İnşaat Mühendisliği Bölümü, 35040 Bornova/İzmir, Türkiye
iv) Professor, University of L'Aquila, Dept. of Civil, Construction-Architectural and Environmental Engineering, Piazzale Ernesto Pontieri 1 – Monteluco di Roio, 67100 L'Aquila, Italy

ABSTRACT

On February 6th, 2023, at 4:17 a.m. local time, a devastating earthquake struck the territories of southeastern Türkiye and northwestern Syria. The moment magnitude recorded for the first strong quake was 7.7. Subsequently, numerous quakes of moment magnitude greater than 3 were recorded in the already affected areas. A further strong quake of magnitude 7.6 at 13:24 local time resulted in further extensive damage in the eleven provinces of Türkiye already hit. This paper focuses on the assessment of the earthquake-induced damage to the built environment observed in Gölbaşı city, located in the Adıyaman province of Türkiye close to the Gölbaşı Lake. The damage data have been collected through an in-situ reconnaissance performed by the Turkish author 10 days after the main seismic events. Analysis of the strong ground motions recorded in Gölbaşı city has been cross-checked with data on geological and subsoil conditions, also integrated with data reported in other studies, and the observed damage mechanisms. The features of the detected damage highlighted the presence of both inertia-induced effects, due mainly to the building vulnerability, and typical damage patterns related to the earthquake-induced liquefaction of the foundation soils, such as punching failure and consolidation settlements. This preliminary assessment shows the significance of this case for the advancement of the knowledge on earthquake-induced liquefaction and traces the route for deeper future studies.

Keywords: February 6th 2023 Türkiye earthquakes, Gölbaşı, damage distribution, liquefaction, subsoil conditions

1 INTRODUCTION

Liquefaction is a phenomenon in which the strength and stiffness of a saturated soil is reduced by earthquake shaking or other rapid loading. Prior to an earthquake, the water pressure is relatively low, however, ground shaking can induce pore water pressure build-up to a point where the soil particles can easily move with respect to each other. When liquefaction occurs, the strength of the soil decreases, and the ability of a soil deposit to support foundations for buildings and bridges is reduced.

Seismically induced cyclic pore water pressure generation and liquefaction may produce several mechanisms of movement in buildings. The main mechanisms of motion can be divided into two classes (Bray and Dashti 2014): shear-induced deformation and volume-induced deformation. The first category includes partial bearing failure under the static load of structures due to strength loss in the foundation soil, resulting in punching settlements or tilting of the structure and cumulative ratcheting foundation displacement induced by cyclic loading near the edges of the foundation. The second mechanism refers to localized volumetric strains during partially drained cyclic loading controlled by transient hydraulic gradients, downward displacement due to sedimentation or solidification after liquefaction or soil structure breakdown, and consolidation-induced volumetric strains as excess pore water pressures dissipate and the soil's effective stress increases (Bray and Dashti 2014).

Several liquefaction-induced building damages have been observed after strong seismic events, such as the 1964 Niigata earthquake in Japan, the 1999 Kocaeli earthquake in Türkiye, the 2010-2011 Canterbury seismic sequence in New Zealand and the 2012 Emilia earthquake in Italy (Di Ludovico et al. 2020). More recently, a devastating event of moment magnitude M_w = 7.7 with epicenter in Pazarcık, followed by a M_w = 7.6 event with epicenter in Elbistan, struck the territories of southeastern Türkiye and northwestern Syria on February 6th, 2023. These events, with more than 11,000 aftershocks, resulted in the loss of more than 59,000 lives and more than 130,000 injuries throughout Türkiye.

Many studies have highlighted the state of the infrastructures in terms of damage throughout Türkiye following these strong earthquakes, analyzing the type

of collapse or damage and the causes related to them (Moug et al. 2023). This study provides an overview of the main damage observed in the city of Gölbaşı, affected by extensive liquefaction-induced damage. The reported data and the related photographic documentation have been collected through an in-situ reconnaissance performed by the Turkish author just 10 days after the occurrence of the main seismic events.

In this regard, after a review of the main features of the February 2023 seismic sequence, with a focus on the two main shakings: Pazarcık and Elbistan earthquakes (section 2), the study focuses on the ground motions recorded at the city of Gölbaşı (section 3) and the geological setting and subsoil conditions of the area (section 4). Then, the observed damage is documented in detail and some of the failure mechanisms identified and critically discussed under the light of the geological and subsoil conditions and intensity of the shakings (section 5). Finally, future perspectives of the study are provided in the conclusions.

2 THE FEBRUARY 2023 TÜRKIYE SEISMIC SEQUENCE

On February 6th, 2023, at 4:17 a.m. local time, a devastating M_w = 7.7 earthquake struck the territories of southeastern Türkiye and northwestern Syria. Subsequently numerous shakings of moment magnitude greater than 4 were recorded in the already affected areas (Fig. 1). The first earthquake, identified as the Pazarcık earthquake, was triggered by a left lateral strike-slip fault within the East Anatolian fault zone, and it was followed by another one, named Elbistan earthquake with M_w = 7.6, which occurred at 1:24 p.m. local time. The effects of two strong seismic events in a very short period led to catastrophic situations in many provinces of Türkiye. Numerous buildings and infrastructures were damaged and many of them collapsed because of the second earthquake. Hatay, Kahramanmaraş, Adıyaman, Malatya, Osmaniye, Gaziantep, Kilis, Şanlıurfa, Diyarbakır, Adana, and Elazığ are the eleven Turkish provinces affected (Fig. 2).

The Department of the Earthquake of the Ministry of Interior of the Turkish government installed a dense seismograph array in the country (AFAD 2023). This network successfully recorded strong ground motions of the February 2023 earthquakes.

To better understand the main characteristics of the Pazarcık earthquake, the Peak Ground Acceleration (PGA) of the three-components of the recorded strong motion: east-west (E-W), north-south (N-S) and vertical (U-D), have been recovered from AFAD (2023) and mapped to inspect their distribution (Fig. 3). To provide an idea of the extension of the affected area, the stations that recorded a range of PGA values from 0.1 to > 1 g (the red ones in Fig. 3) cover an area of around 58460 km^2 (Fig. 3a), 54127 km^2 (Fig. 3b) and 16983 km^2 (Fig. 3c), while for the PGA range 0.06-0.1 g (the orange ones in Fig. 3) the area covered is around 79995 km^2 (Fig. 3a), 68236 km^2 (Fig 3b) and 58260 km^2 (Fig. 3c). Similarly, for the Elbistan earthquake the recorded PGA components (E-W, N-S and U-D) have been mapped in Fig. 4 (AFAD 2023). The covered area for PGA values from 0.1 to > 1 g is around 22860 km^2 (Fig. 4a), 19008 km^2 (Fig. 4b) and 8485 km^2 (Fig. 4c), while for the PGA range 0.06-0.1 g the covered area is around 46269 km^2 (Fig. 4a), 42200 km^2 (Fig. 4b) and 18593 km^2 (Fig. 4c). For the first shaking, the affected area for PGA from 0.1 to > 1 g, which can be considered the range of interest from an engineering point of view, is more than 2.5 times larger than for the second event, while the affected area for PGA in the range 0.06-0.1 g is more than 1.5 times larger than that affected by the second event.

In both seismic scenarios, the city of Gölbaşı is in the most affected epicentral areas (Figs 3 and 4). In addition, a recording station located in the city (station code 0280) recorded the Pazarcık seismic event (Fig. 3). The PGA distribution in Fig. 3 shows that the PGA values recorded in Gölbaşı represent an anomaly respect to the surroundings stations, with recorded values much lower especially for the E-W and U-D components (green triangles in Figs 3a and 3c).

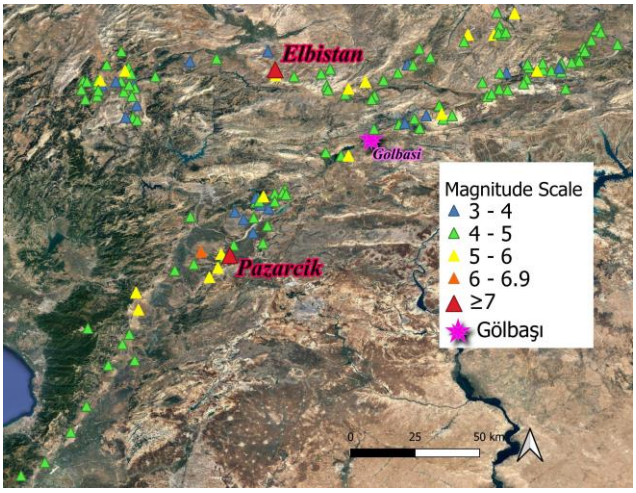

Fig. 1. Location of epicenters with magnitude of the seismic sequence started on February 6th, 2023 (data from AFAD 2023).

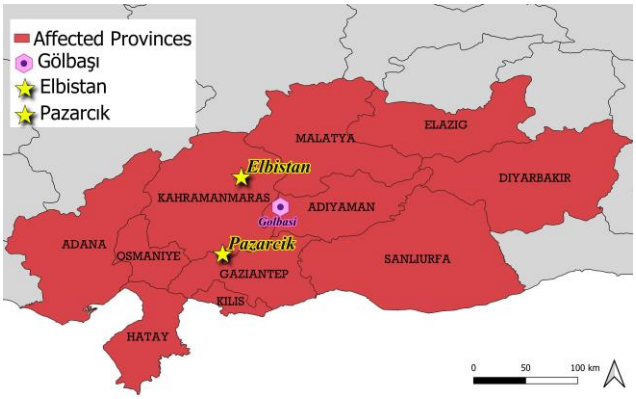

Fig. 2. The eleven provinces most affected by the February 6th, 2023 earthquakes.

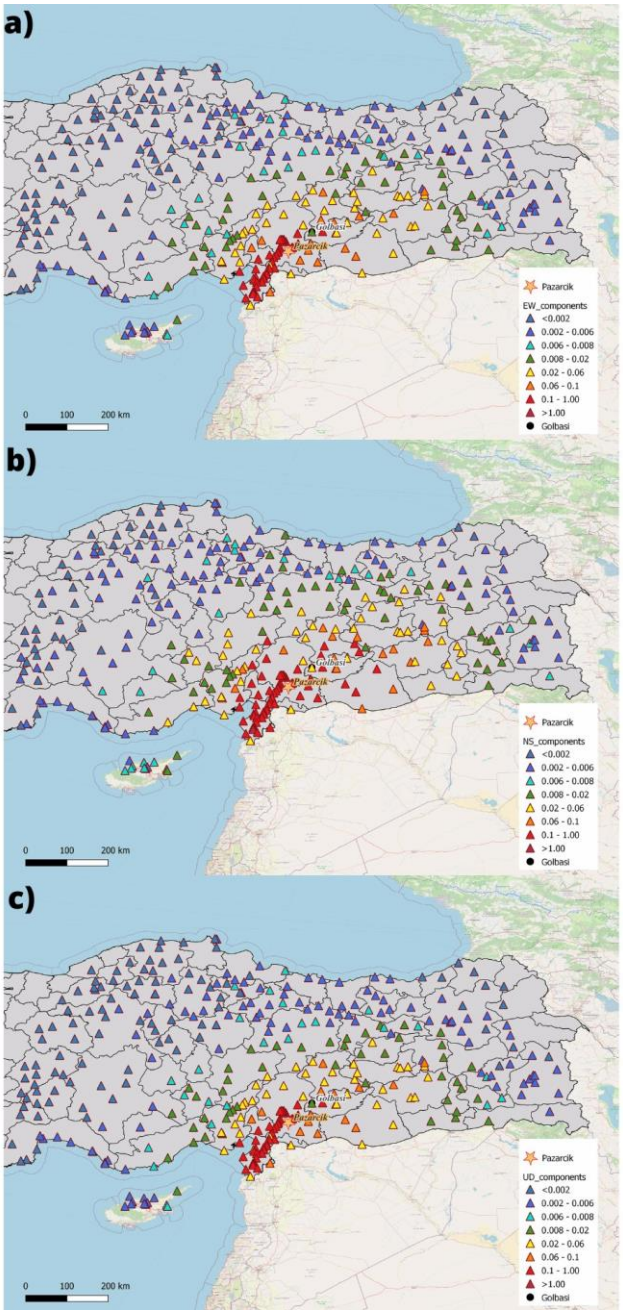

Fig. 3. Distribution of PGA (g) recorded for the Pazarcık earthquake: (a) E-W, (b) N-S and (c) U-D component (data from AFAD 2023).

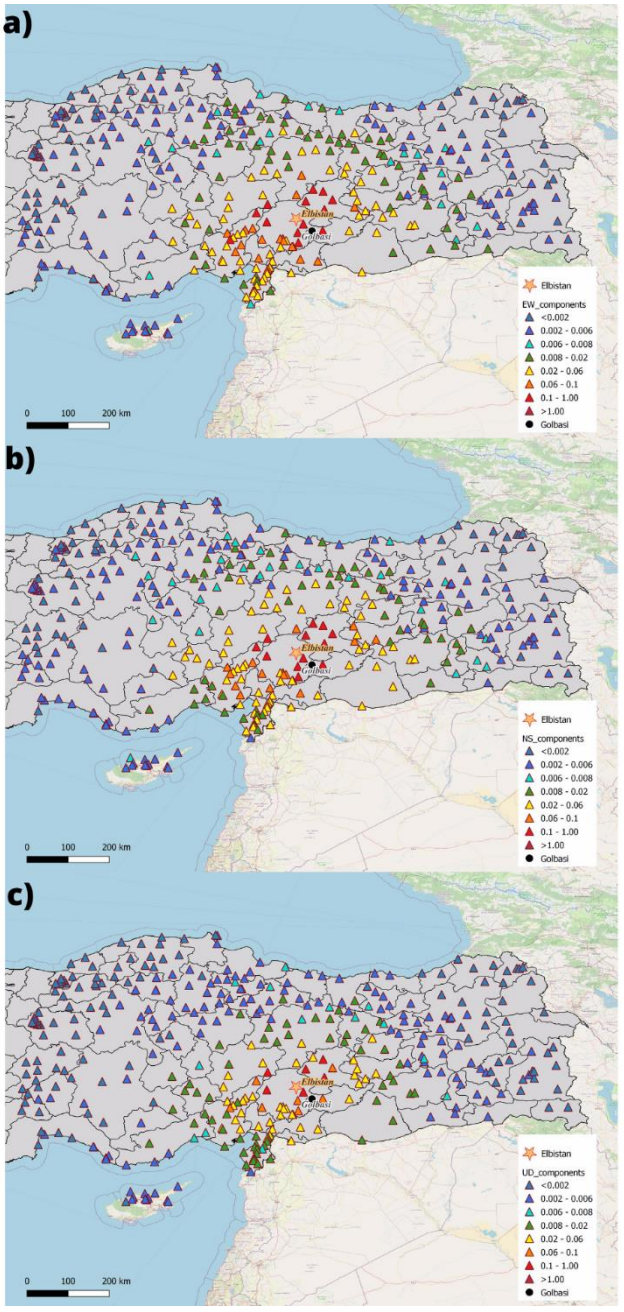

Fig. 4. Distribution of PGA (g) recorded for the Elbistan earthquake: (a) E-W, (b) N-S and (c) U-D component (data from AFAD 2023).

No considerations can be made on the PGA recorded in Gölbaşı after the Elbistan earthquake, because the recorded signals are not available from AFAD (2023).

3 RECORDED MOTIONS IN GÖLBAŞI CITY

The city of Gölbaşı, of about 34000 inhabitants, is located near the Gölbaşı Lake, in the Adıyaman province (Figs 2 and 5). After the February 6th, 2023 earthquakes, observations made in the Gölbaşı district revealed very intense structural damage and ground deformations, such as total and differential settlements due to liquefaction. In addition, lateral spreading was also observed in some areas (Moug et al. 2023).

Fig. 5 shows the strong motion recording stations located in the surrounding of Gölbaşı with the related subsoil classification according to the Eurocode 8 (2005), and the main faults in the area. Only one station, "Besni", is classified in the subsoil class A; unfortunately, no records are available for both seismic events. Conversely, the station named "Tut" that recorded both seismic events has no information regarding the subsoil class. However, the majority of the recording stations around the city of Gölbaşı have a subsoil class B, i.e., "deposits of very dense sand, gravel, or very stiff clay, at least several tens of meters in

thickness, characterized by a gradual increase of mechanical properties with depth" according to the Eurocode 8 (2005).

Tables 1 and 2 summarize the values of PGA (g) recorded by different stations near Gölbaşı at variable epicentral distance (R_{epi}) for the Pazarcik and Elbistan earthquakes, respectively.

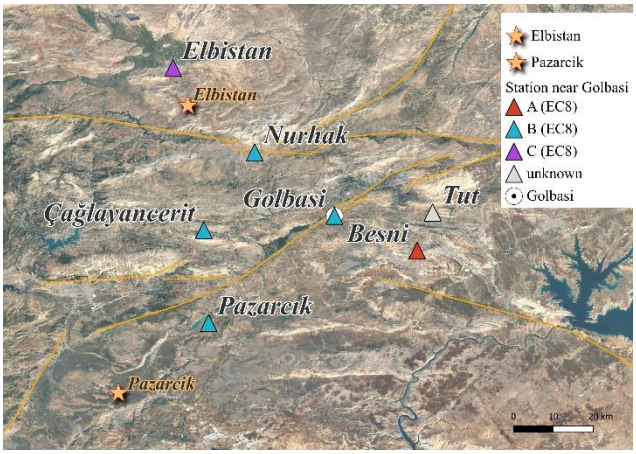

Fig. 5. Distribution of the strong motion recording stations near Gölbaşı and main faults (in yellow).

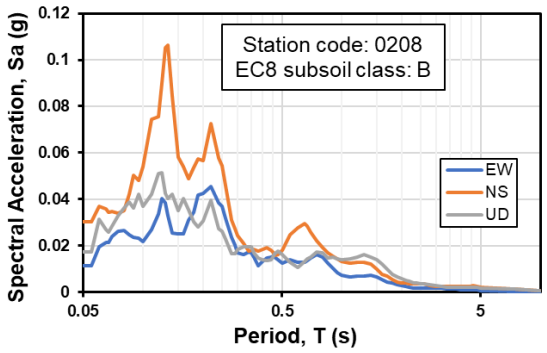

Fig. 6. Response spectra of Pazarcık earthquake by station 0280.

Table 1. PGA (g) recorded by stations near Gölbaşı for Pazarcik earthquake (AFAD 2023).

Station	Soil Type	E-W	N-S	U-D	R_{epi} (km)
Nurhak	B	0.02	0.023	0.034	82.68
Çağlayancerit	B	0.33	0.36	0.18	55.32
Pazarcık	B	2.08	2.06	1.61	31.42
Gölbaşı	B	0.014	0.03	0.017	77.26

Table 2. PGA (g) recorded by stations near Gölbaşı for Elbistan earthquake (AFAD 2023).

Station	Soil Type	E-W	N-S	U-D	R_{epi} (km)
Nurhak	B	0.4	0.34	0.62	21.43
Çağlayancerit	B	0.14	0.198	0.074	38.21
Pazarcık	B	0.21	0.164	0.09	67.35

Table 3. Ground motion parameters of the Pazarcık earthquake recorded by station 0280 located in Gölbaşı (AFAD 2023).

Component	AI (cm/s)	HI (cm)	T_{90} (s)	PGA (g)	PGV (cm/s)	PGD (cm)	S_a (1s) (g)
E-W	0.1042	3.4281	2.75	0.014	0.945	0.236	0.0072
N-S	0.2396	4.6673	3.22	0.031	1.715	1.151	0.0133
U-D	0.153	4.4866	3.73	0.017	1.416	1.313	0.0137

Fig. 6 shows the response spectra of the three components of the Pazarcık earthquake recorded by the Gölbaşı station (data from AFAD 2023, as available on May 2023). The peak and integral parameters of the ground motion (Arias Intensity AI, Housner Intensity HI, duration T_{90}, Peak Ground Acceleration PGA, Peak Ground Velocity PGV, Peak Ground Displacement PGD, Spectral Acceleration S_a) are reported in Table 3. From the above data the intensity of the recorded ground motion appears extremely low, and not consistent with the observed damage. However, the waveform data is cut off after a few seconds, and it is clear that the main motions were not recorded compared to the records of surrounding stations. Therefore, the reliability of these data is doubtful and the authors do not consider them as representative of the Pazarcık ground motion in Gölbaşı.

4 GEOLOGICAL SETTING AND SUBSOIL CONDITIONS IN GÖLBAŞI

Fig. 7 shows the geological map of Gölbaşı city and surrounding areas. The geological formations are composed of a variety of rock types, including sedimentary (limestone, sandstone, shale), metamorphic (marble, schist) and igneous rocks (basalt, andesite).

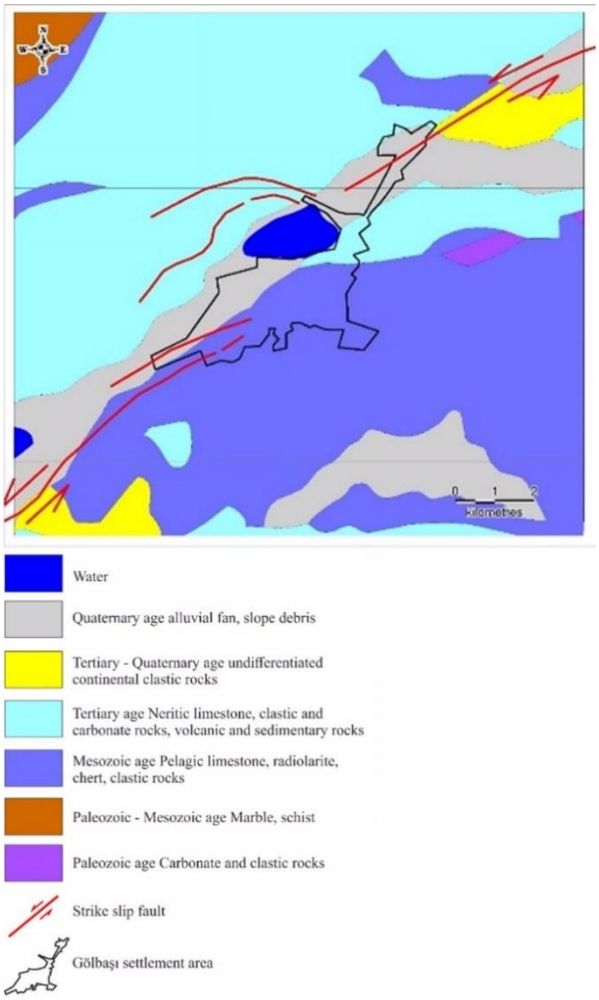

Fig. 7. Geological map of Gölbaşı city and surrounding areas.

Limestone, as encountered in many parts of Türkiye, shows karst features, characterized by sinkholes, caves, and underground flow formed by the dissolution of limestone by water. The presence of underground aquifers within certain geological formations is a reason for the significant impact of groundwater in the region. Gölbaşı city boundaries comprises many lakes and reservoirs. These lacustrine environments are often formed for the purpose of water storage and hydroelectric power generation. The bottoms of these reservoirs are typically composed of lacustrine soils, consisting of clay, silt, sand, and organic soils. Based on available information, in Gölbaşı city the topmost portion of the soil profile is typically composed of alternating layers of clay, sand and gravel. The groundwater table is close to the ground surface.

Moug et al. (2023) collected and analyzed some samples of ejected soil in the area shown in Fig. 8. Through this analysis, it was possible to determine the Atterberg limits and the grain size distribution. The fines content varies between 18% and 52% and the plasticity index (PI) is between 9% and 14% (Moug et al. 2023). It is interesting to note that the collected samples fall within two different geological areas.

5 DAMAGE AND LIQUEFACTION OBSERVATIONS IN GÖLBAŞI

The strong earthquakes that hit the area on February 6th, 2023 produced widespread damage and evidence of liquefaction. Fig. 9 provides an overview of the observations collected by the in-situ reconnaissance performed by the Turkish author 10 days after the main seismic events (pink symbols), further integrated with the lateral spreading observations (yellow symbols) reported by GEER (2023). Fig. 10 focuses on the observed building damage in the city, by showing several pictures of the observed failure mechanisms.

By analyzing the images observed in Gölbaşı after the earthquakes (Figs 9 and 10), a significant amount of lateral spreading, liquefaction and differential settlements can be observed in the city and in many locations near the lake. Manifestations of ground failure with evidence of liquefaction-induced ejecta of silty/clayey sands (e.g., images 6, 19), as well as rigid rotation of shallow foundations with consequent tilting of the building (e.g., image 15), can be observed. The presence of inertia-induced effects, failures due to the out-of-plane mechanisms of walls or in-plane diagonal cracks (Di Ludovico et al. 2020) commonly associated to strong earthquake (e.g., images 1, 16), combined with the liquefaction-induced damages, can also be observed. For liquefaction, the damage caused by inertial forces is mostly absent, because liquefaction works as a natural isolation system for the superstructure (Di Ludovico et al. 2020). This was also experienced by field reconnaissance of the Turkish author: many severely damaged structures exposed to large settlements due to

Fig. 8. Locations of ejecta sampled by Moug et al. (2023) in Gölbaşı on 30th March, 2023.

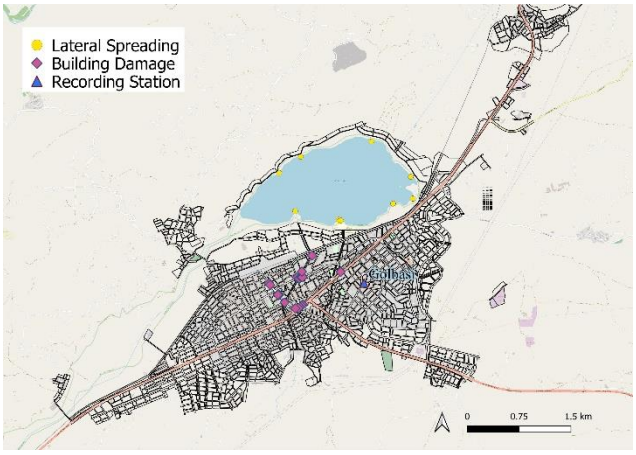

Fig. 9. Location of observed evidence of liquefaction and building damage (lateral spreading data retrieved from GEER 2023).

liquefaction were observed in Gölbaşı (e.g., image 13). Typical damage patterns related to the earthquake-induced liquefaction of the foundation soils, such as punching failure, consolidation settlements (e.g., images 5, 9, 20) and lateral collapses of buildings (e.g., image 7), were also observed.

6 CONCLUSIONS

This study documents the damage observed in the Gölbaşı city after the February 6th, 2023 earthquakes. Due to the presence of both predisposing and triggering conditions for the occurrence of liquefaction (i.e., shallow saturated sand deposits, severe ground motions), it can be concluded that the intense damage pattern observed in the city is mainly related to liquefaction-induced damage. Major sources of uncertainty for the quantitative assessment of the observed liquefaction phenomena, as to the information available to the authors, are related to: (i) lack of geotechnical characterization data, and (ii) anomalies in the ground motion recordings at the Gölbaşı station, which are not considered reliable. Future study will address more accurate investigation of the soil conditions and determination of the seismic input.

Fig. 10. Observed building damage due to liquefaction as collected in the field reconnaissance performed by the Turkish author in Gölbaşı.

ACKNOWLEDGEMENTS

The authors thank Professor Cem Kıncal from Dokuz Eylül University, Department of Geology, for his kind contribution in mapping of Gölbaşı city and periphery.

REFERENCES

1) AFAD (2023): PRESS BULLETIN-36 about the Earthquake in Kahramanmaraş, https://en.afad.gov.tr/press-bulletin-36-about-the-earthquake-in-kahramanmaras (accessed 18 May 2023)
2) Bray, J. and Dashti, S. (2014): Liquefaction-induced building movements, *Bulletin of Earthquake Engineering*, 12, 1129-1156, https://doi.org/10.1007/s10518-014-9619-8
4) Di Ludovico, M., Chiaradonna, A., Bilotta, E., Flora, A. and Prota, A. (2020): Empirical damage and liquefaction fragility curves from 2012 Emilia earthquake data, *Earthquake Spectra*, 36(2), 507-536, https://doi.org/10.1177/8755293019891713
5) Eurocode 8 (2005): EN 1998-1 Design of structures for earthquake resistance — Part 1: General rules, seismic actions and rules for buildings.
6) GEER (2023): February 6, 2023 Türkiye Earthquakes: Report on Geoscience and Engineering Impacts. GEER Association Report 082, https://doi.org/10.18118/G6PM34
7) Moug, D., Bassal, P., Bray, J.D., Çetin, K.Ö., Kendir, S.B., Şahin, A., Çakır, E., Söylemez, B. and Ocak, S. (2023): February 6, 2023 Türkiye Earthquakes: GEER Phase 3 Team Report on Selected Geotechnical Engineering Effects, GEER Association Report 082-S1, https://doi.org/10.18118/G6F379